TECHNISCHE MECHANIK, 31, 1, (2011), 15 – 24
submitted: November 17, 2009

Self-Excitation Mechanisms in Paper Calenders Formulated as a Stability Problem

G. Spelsberg-Korspeter, D. Hochlenert, P. Hagedorn

Abstract

In one of the last stages of paper production the surface of the paper is refined in calenders. The paper is compressed in the nip by rollers which sometimes tend to exhibit self-excited vibrations. These vibrations may lead to wear and dramatically reduce the durability of the expensive rollers. The reason for the self-excited vibrations is to be found in the interaction of the rollers with the paper. The interaction process in the nip is very complex and has not been completely understood from a mechanical point of view. The purpose of this paper is to develop simple mechanical models of the nip which can lead to an explanation of the phenomenon.

1 Introduction

The process of paper calendering is one of the last steps in paper production. In the nip between two calender rolls, the coarse paper is heated and compressed in order to refine its surface, making it suitable for modern printers or further applications. A detailed description of the process can be found in (1). Due to the interaction of the paper and the rollers, self-excited vibrations may arise, leading to wear and decreasing the durability of the rollers.

Different excitation mechanisms are proposed in the literature. One line of reasoning suggests self-excited vibrations due to delay terms in the equations of motion caused by wear (cf. (2) and the references therein). Another explanation is sought in the occurrence of nonconservative forces in the nip, transferring energy from the rotation of the rollers to vibrations of the system.

Taking into account nonconservative forces in the nip, self-excitation can be substantiated without heuristic wear models. In (3; 4) BROMMUNDT aims in this direction and models the rollers as rotating elastic rings. Using a simple paper model and assuming slip between the paper and the rollers, the nonlinear equations of motion of the system are derived and self-excitation is shown by numerical integration of the equations of motion.

The purpose of this paper is to develop models which allow for a systematic stability analysis, without having to perform a numerical integration of the equations of motion. In a first step, the rollers are modeled as rigid cylinders and the paper is considered as inextensible in the horizontal direction. This causes slip between the paper and the rollers, yielding a similar excitation mechanism as in (3; 4). Since it is doubtful weather slip between the paper and the rollers is a realistic assumption, a paper model which allows for shear deformations is considered in a next step. It is shown that self-excitation is possible in this case as well.

2 Single rigid roller with inextensible paper

In this section, a single rigid roller in frictional contact with inextensible paper is considered (Figure 1). In a first step for symmetry reasons a model of only one rigid roller in contact with the paper web is considered and the velocity of the mid surface of the paper is prescribed. As a consequence all parameters correspond to half of the paper thickness. The roller is supported by two prestressed linear springs (stiffness k_x, k_y, prestress F_{x0}, F_{y0}) and rotates at constant angular velocity Ω. The paper, represented by an elastic foundation (bedding coefficient $k_{\mathrm{b}y}$), moves at constant velocity v in horizontal direction (Figure 2). Each material point characterized by the coordinate ξ on the surface of the paper undergoes displacements $u(\xi, t)$ perpendicular to the neutral inextensible fibre of the paper only. A shear deformation of the paper is thus neglected. The points in the nip are characterized by the coordinate s defined in Figure 1. In the nip, the paper is compressed and then leaves the nip at its narrowest point,

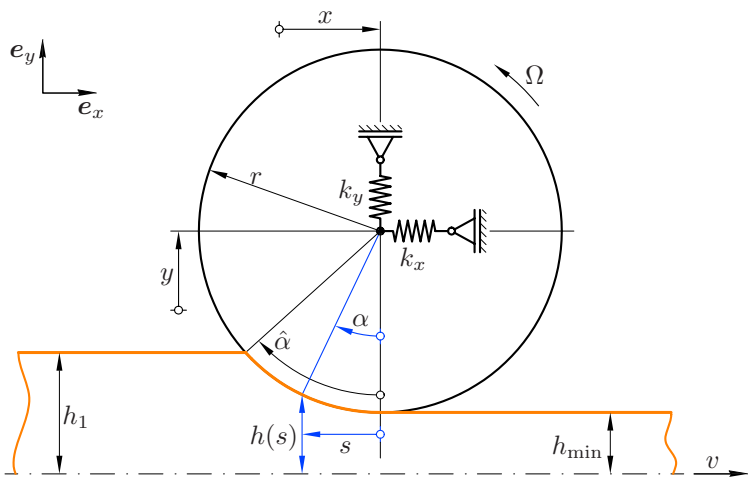

Figure 1: Rigid roller in contact with idealized paper

maintaining its minimum thickness $h_{\min}$. The truncation at the end of the nip takes care of the plastic deformation of the paper.

In order to keep the model simple, the deformation process of the paper in the nip is modeled as quasi-stationary. This means that the forces acting on the roller are calculated from a stationary process arising in the current dynamical state of the system. This assumption is justified taking into account the fact that the period of the vibration is about seventy times the time a material point of the paper spends in the nip. The ratio is calculated from the parameters used for the calculations in section 3 with a paper velocity of 800 m/s and a frequency of the resulting unstable mode of approximately 30 Hz. For a frequency of 200 Hz, the period of the vibration is still over ten times larger than the time a material point of the paper spends in the nip. Therefore the stationary process is reached almost instantaneously (i.e. in a small fraction of the time a point spends in the nip). Regarding the fact that the nip angle is about one degree, this is also intuitively clear. Without the assumption of a quasi-stationary process, the equations of motion would not only depend on the current state of the system but also on the loading history of the elements of the paper after entering the nip.

The two coordinates of freedom x and y of the roller center are measured from the prestressed steady state configuration characterized by a paper thickness h_0 at the narrowest point of the nip. The thickness of the paper at a point defined by the coordinate s in the nip is given by

$$h(s, y) = r + h_{\min} - \sqrt{r^2 - s^2} \tag{1}$$

where

$$h_{\min} = h_0 + y \tag{2}$$

is the thickness at the end of the nip. The relation $s = r \sin\alpha$ yields

$$h(\alpha, y) = h_0 + r(1 - \cos\alpha) + y \tag{3}$$

and with $h(\hat{\alpha}, y) = h_1$ one obtains

$$\cos\hat{\alpha} = 1 - \frac{h_1 - h_0 - y}{r}\,. \tag{4}$$

Excluding shear deformations of the paper there is at most one point of vanishing relative velocity between the paper and the roller, as follows from kinematical reasons. If the relation

$$\dot{x} + \Omega r \cos\alpha_{\mathrm{st}} = v \tag{5}$$

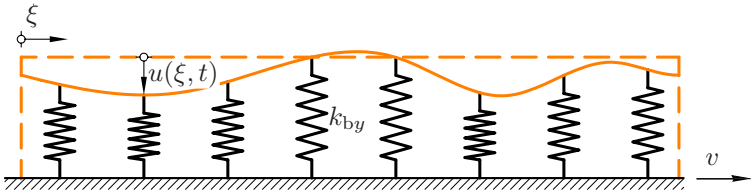

Figure 2: Paper model (inextensible and without shear deformation)

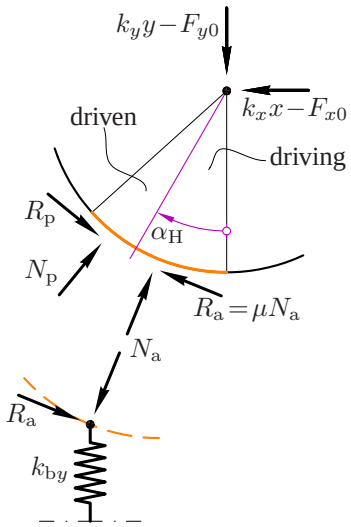

Figure 3: Contact forces between the roller and the paper

holds for some value of α_st with $0 < \alpha_\mathrm{st} < \hat{\alpha}$, this does in fact correspond to a point of vanishing relative velocity in the nip. At all other contact points between roller and paper there is sliding friction and the relative velocity determines the direction of the friction forces (cf. Figure 3). In the region $\alpha < \alpha_\mathrm{st}$ indicated by the subscript a the roller *actively* drives the paper; in the region $\alpha > \alpha_\mathrm{st}$ indicated by the subscript p the roller is driven by the paper (p stands for a roller *passively* driven by the paper).

Using COULOMB's law, the distributed contact forces at a contact point in the nip parameterized by α can be calculated from a force balance at a segment of the paper as

$$N_\mathrm{a} = \frac{k_{\mathrm{b}y}(h_1 - h)}{\cos\alpha + \mu \sin\alpha}\,, \qquad R_\mathrm{a} = \mu N_\mathrm{a}\,, \tag{6a}$$

$$N_\mathrm{p} = \frac{k_{\mathrm{b}y}(h_1 - h)}{\cos\alpha - \mu \sin\alpha}\,, \qquad R_\mathrm{p} = \mu N_\mathrm{p}\,. \tag{6b}$$

From NEWTON's law, the equations of motion of the roller can be derived as

$$m\ddot{x} + k_x x = F_{x0} + \int_0^{\alpha_\mathrm{st}} N_\mathrm{a}(\sin\alpha - \mu\cos\alpha) r \cos\alpha \,\mathrm{d}\alpha + \int_{\alpha_\mathrm{st}}^{\hat{\alpha}} N_\mathrm{p}(\sin\alpha + \mu\cos\alpha) r \cos\alpha \,\mathrm{d}\alpha\,, \tag{7a}$$

$$m\ddot{y} + k_y y = F_{y0} + \int_0^{\hat{\alpha}} k_{\mathrm{b}y}(h_1 - h) r \cos\alpha \,\mathrm{d}\alpha\,, \tag{7b}$$

where the distributed contact forces were summed over the nip by integration. The forces acting at the point of sticking do not change the value of the integral, since they occur on a set of measure zero.

To determine the stability of the trivial solution, the equations of motion are linearized with respect to x, y, $\dot{x}$, $\dot{y}$ around the steady state configuration. From (4) and (5) one obtains the functions $\hat{\alpha}(y)$, $\alpha_\mathrm{st}(\dot{x})$ and the boundaries of the integrals in (7) have to be differentiated according to LEIBNIZ's rule. For the case $0 < \alpha_\mathrm{st}(0) < \hat{\alpha}(0)$, i.e. in which a point of vanishing relative velocity exists in the nip, the linearized equations of motion read

$$\begin{bmatrix} m & 0 \\ 0 & m \end{bmatrix} \begin{bmatrix} \ddot{x} \\ \ddot{y} \end{bmatrix} + \begin{bmatrix} f_d & 0 \\ 0 & 0 \end{bmatrix} \begin{bmatrix} \dot{x} \\ \dot{y} \end{bmatrix} + \begin{bmatrix} k_x & k_{\mathrm{b}y} r f_{k1} \\ 0 & k_y + k_{\mathrm{b}y} r \sin\hat{\alpha}_0 \end{bmatrix} \begin{bmatrix} x \\ y \end{bmatrix} = \begin{bmatrix} 0 \\ 0 \end{bmatrix} \tag{8}$$

with the abbreviations $\hat{\alpha}_0 = \hat{\alpha}(0)$, $\alpha_{\mathrm{st}0} = \alpha_\mathrm{st}(0)$ and

$$f_d = \mu k_{\mathrm{b}y} \frac{h_1 - h_0 - r(1 - \cos\alpha_{\mathrm{st}0})}{\Omega} \frac{\cos\alpha_{\mathrm{st}0} + \cos 3\alpha_{\mathrm{st}0}}{\sin\alpha_{\mathrm{st}0}\left(\cos\alpha_{\mathrm{st}0} - \mu^2 \sin\alpha_{\mathrm{st}0}\right)}\,, \tag{9a}$$

$$f_{k1} = \int_0^{\alpha_{\mathrm{st}0}} \frac{\sin\alpha - \mu\cos\alpha}{\cos\alpha + \mu\sin\alpha} \cos\alpha \,\mathrm{d}\alpha + \int_{\alpha_{\mathrm{st}0}}^{\hat{\alpha}_0} \frac{\sin\alpha + \mu\cos\alpha}{\cos\alpha - \mu\sin\alpha} \cos\alpha \,\mathrm{d}\alpha\,. \tag{9b}$$

It is interesting to note that a positive semidefinite damping matrix arises due to the derivative of the integral boundaries α_{st}. The damping term is absent if the relative velocity between the paper and the roller does not vanish at any point in the nip. In this case the linearized equations of motion are

$$\begin{bmatrix} m & 0 \\ 0 & m \end{bmatrix} \begin{bmatrix} \ddot{x} \\ \ddot{y} \end{bmatrix} + \begin{bmatrix} k_x & k_{\mathrm{b}y} r\, f_{k2} \\ 0 & k_y + k_{\mathrm{b}y} r \sin\hat{\alpha}_0 \end{bmatrix} \begin{bmatrix} x \\ y \end{bmatrix} = \begin{bmatrix} 0 \\ 0 \end{bmatrix} \tag{10}$$

with

$$f_{k2} = \int_0^{\hat{\alpha}_0} \frac{\sin\alpha \mp \mu\cos\alpha}{\cos\alpha \pm \mu\sin\alpha} \cos\alpha \,\mathrm{d}\alpha \,, \tag{11}$$

where the upper sign holds for the roller actively driving the paper, i.e. $v < \Omega r \cos\alpha$, and the lower sign holds for the roller being passively driven by the paper, i.e. $v > \Omega r \cos\alpha$ over the whole nip.

Both, (8) and (10), feature a one-sided coupling due to the truncation of the paper at the end of the nip and due to the fact that the contact forces depend exclusively on y and not on x. The asymmetry of the stiffness matrix holds even for $\mu = 0$. This shows that the nonconservative character of the restoring term is not exclusively due to friction but originates from the relative motion of the material points of the paper and the roller which contact each other in the nip. This is a major difference compared to models in which the nip is modeled as a single spring connecting two material points leading to symmetric matrices.

Considering exactly the present equations of motion, instability of the trivial solution, i.e. self-excitation, only occurs for (10) if the diagonal elements of the stiffness matrix are equal. Double eigenvalues then arise leading to JORDAN blocks of the corresponding first order system. However, additional small coupling of the equations of motion by damping or other neglected effects, can instantaneously cause instability. In this context we note that we have not introduced damping in the suspension of the rollers which certainly will yield a coupling of the linearized equations of motion. In this context, the model of a single rigid roller with inextensible paper might indicate the origin of a possible self-excitation, but the restriction to one roller possibly hides important effects, such as an additional coupling of the equations of motion. Therefore, an extended model consisting of two rollers is considered in the following section.

3 Two rigid rollers with inextensible paper

The model depicted in Figure 4 consists of two rollers (radii r_i, degrees of freedom x_i, y_i, $i = 1, 2$) and the paper web modeled as in the previous section. The speed of rotation of the rollers is prescribed by Ω_1 and Ω_2 respectively and the velocity of the paper is $v\boldsymbol{e}_t$ with constant magnitude v.

In the steady state all displacements are zero, the centers of the rollers are aligned vertically and the paper has the thickness h_0 at the end of the nip ($s = 0$). In the dynamic case, the thickness $h_{\min}$ of the paper at ($s = 0$) follows from

$$(x_2 - x_1)^2 + (r_1 + r_2 + h_0 + y_1 + y_2)^2 = (r_1 + r_2 + h_{\min})^2. \tag{12}$$

The trigonometric functions of the angle α_0 corresponding to $s = 0$ are

$$\tan\alpha_0 = \frac{x_2 - x_1}{r_1 + r_2 + h_0 + y_1 - y_2}, \qquad \sin\alpha_0 = \frac{x_1 - x_2}{r_1 + r_2 + h_{\min}} \tag{13}$$

and the thickness of the paper as a function of s is

$$h = r_1 + r_2 + h_{\min} - \sqrt{r_1^2 - s^2} - \sqrt{r_2^2 - s^2}\,. \tag{14}$$

In the following, it will be convenient to express the paper thickness h as a function of the angles α_1 and α_2 as

$$h = h_{\min} + r_1(1 - \cos(\alpha_1 - \alpha_0) + r_2(1 - \cos(\alpha_2 + \alpha_0))), \tag{15}$$

where α_1 and α_2 are defined in Figure 4 and are related to s by

$$s = r_1 \sin(\alpha_1 + \alpha_0) = r_1(\sin\alpha_1 \cos\alpha_0 + \cos\alpha_1 \sin\alpha_0), \tag{16a}$$

$$s = r_2 \sin(\alpha_2 - \alpha_0) = r_2(\sin\alpha_2 \cos\alpha_0 - \cos\alpha_2 \sin\alpha_0). \tag{16b}$$

The angles $\hat{\alpha}_1$ and $\hat{\alpha}_2$ can be determined from (15) using the condition $h(\hat{\alpha}_i) = h_1$ $(i = 1, 2)$.

In order to calculate the contact forces between the paper and the rollers sketched in Figure 5 one needs the velocities of points on the surface of the roller given by

$$\boldsymbol{v}_1(\alpha_1) = \dot{x}_1 \boldsymbol{e}_x + \dot{y}_1 \boldsymbol{e}_y + \Omega_1 \boldsymbol{e}_z \times r_1(-\sin\alpha_1 \boldsymbol{e}_x - \cos\alpha_1 \boldsymbol{e}_y), \tag{17a}$$

$$\boldsymbol{v}_2(\alpha_2) = \dot{x}_2 \boldsymbol{e}_x + \dot{y}_2 \boldsymbol{e}_y - \Omega_2 \boldsymbol{e}_z \times r_2(-\sin\alpha_2 \boldsymbol{e}_x + \cos\alpha_2 \boldsymbol{e}_y). \tag{17b}$$

As in the previous section there is at most one point of vanishing relative velocity between each roller and paper

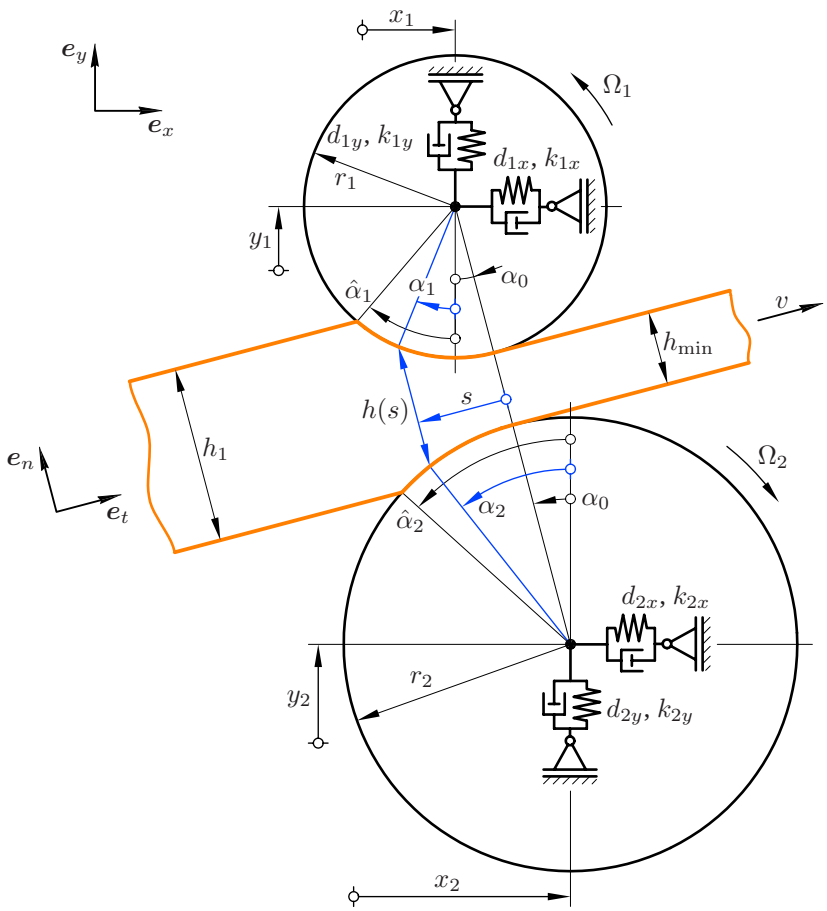

Figure 4: Two rigid rollers in contact with idealized paper

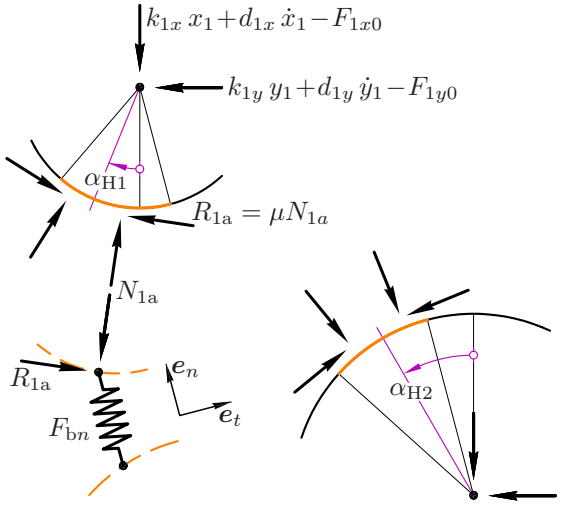

Figure 5: Contact forces between the rollers and the paper (F_{bn} denotes the force in the paper element)

defined by the conditions

$$\boldsymbol{v}_1(\alpha_{\mathrm{st}1}) \cdot \boldsymbol{e}_t = v, \tag{18a}$$
$$\boldsymbol{v}_2(\alpha_{\mathrm{st}2}) \cdot \boldsymbol{e}_t = v. \tag{18b}$$

If at least one of these conditions is fulfilled for

$$-\alpha_0 < \alpha_{\mathrm{st}1} < \hat{\alpha}_1, \tag{18c}$$
$$\alpha_0 < \alpha_{\mathrm{st}2} < \hat{\alpha}_2, \tag{18d}$$

respectively, there is indeed a point of sticking between the paper and the corresponding roller, and the friction force inverts its direction in the nip. The distributed contact forces can be calculated from a force balance at an infinitesimal element of the paper and read

$$N_{1\mathrm{a}} = \frac{F_{\mathrm{b}n}(\alpha_1)}{\cos(\alpha_1+\alpha_0) + \mu\sin(\alpha_1+\alpha_0)}, \qquad R_{1\mathrm{a}} = \mu N_{1\mathrm{a}}, \tag{19a}$$
$$N_{1\mathrm{p}} = \frac{F_{\mathrm{b}n}(\alpha_1)}{\cos(\alpha_1+\alpha_0) - \mu\sin(\alpha_1+\alpha_0)}, \qquad R_{1\mathrm{p}} = \mu N_{1\mathrm{p}} \tag{19b}$$

for the upper and

$$N_{2\mathrm{a}} = \frac{F_{\mathrm{b}n}(\alpha_2)}{\cos(\alpha_2-\alpha_0) + \mu\sin(\alpha_2-\alpha_0)}, \qquad R_{2\mathrm{a}} = \mu N_{2\mathrm{a}}, \tag{19c}$$
$$N_{2\mathrm{p}} = \frac{F_{\mathrm{b}n}(\alpha_2)}{\cos(\alpha_2-\alpha_0) - \mu\sin(\alpha_2-\alpha_0)}, \qquad R_{2\mathrm{p}} = \mu N_{2\mathrm{p}} \tag{19d}$$

for the lower roller, where the subscripts a and p refer again to the roller actively driving the paper and the roller being passively driven by the paper, respectively. The expression $F_{\mathrm{b}n}(\alpha)$ denotes the force in a paper element in $\boldsymbol{e}_n$-direction at position α. It represents the material behavior of the paper and can be prescribed as an arbitrary function of α. Having in mind the elastic foundation, a straightforward choice is the dependence on the paper thickness

$$F_{\mathrm{b}n}(\alpha_{1,2}) = f(h(\alpha_{1,2})). \tag{20}$$

The equations of motion then follow from NEWTON's law. For the upper roller they are

$$\begin{aligned} m_1\ddot{x}_1 + k_{1x}\,x_1 + d_{1x}\,\dot{x}_1 = F_{1x0} &+ \int_{-\alpha_0}^{\alpha_{\mathrm{st}1}} \Big(N_{1\mathrm{a}}(\sin\alpha_1 - \mu\cos\alpha_1) r_1 \cos\alpha_1\Big)\,\mathrm{d}\alpha_1 \\ &+ \int_{\alpha_{\mathrm{st}1}}^{\hat{\alpha}_1} \Big(N_{1\mathrm{p}}(\sin\alpha_1 + \mu\cos\alpha_1) r_1 \cos\alpha_1\Big)\,\mathrm{d}\alpha_1, \end{aligned} \tag{21a}$$

$$\begin{aligned} m_1\ddot{y}_1 + k_{1y}\,y_1 + d_{1y}\,\dot{y}_1 = F_{1y0} &+ \int_{-\alpha_0}^{\alpha_{\mathrm{st}1}} \Big(N_{1\mathrm{a}}(\cos\alpha_1 + \mu\sin\alpha_1) r_1 \cos\alpha_1\Big)\,\mathrm{d}\alpha_1 \\ &+ \int_{\alpha_{\mathrm{st}1}}^{\hat{\alpha}_1} \Big(N_{1\mathrm{p}}(\cos\alpha_1 - \mu\sin\alpha_1) r_1 \cos\alpha_1\Big)\,\mathrm{d}\alpha_1. \end{aligned} \tag{21b}$$

For the lower roller they have a similar form. The equations of motion can be linearized around the steady state equilibrium position for given Ω_1, Ω_2 and v. With the vector of generalized coordinates

$$\boldsymbol{q} = \begin{bmatrix} x_1 & y_1 & x_2 & y_2 \end{bmatrix}^{\mathsf{T}} \tag{22}$$

one obtains the functions $\alpha_0(\boldsymbol{q})$, $\hat{\alpha}_{1,2}(\boldsymbol{q})$ and $\alpha_{\mathrm{st}1,2}(\boldsymbol{q},\dot{\boldsymbol{q}})$, which means that the integral boundaries in (21) have to be differentiated in the linearization. The linearized equations of motion thus have the form

$$\boldsymbol{M}\ddot{\boldsymbol{q}} + \boldsymbol{D}\dot{\boldsymbol{q}} + (\boldsymbol{K}+\boldsymbol{N})\boldsymbol{q} = \boldsymbol{0} \tag{23}$$

with constant coefficient matrices and the stability of the trivial solution can be studied using the exponential ansatz $\boldsymbol{q}(t) = \hat{\boldsymbol{q}}e^{\lambda t}$ yielding the characteristic equation

$$\det(\lambda^2\boldsymbol{M} + \lambda\boldsymbol{D} + \boldsymbol{K} + \boldsymbol{N}) = 0.$$

In the following, the parameters of Table 1 communicated by VAN HAAG (5) are employed, corresponding to the

$m_1 = 6447\,\text{kg}$	$m_2 = 16114\,\text{kg}$	$h_1 = 150\,\mu\text{m}$
$\omega_1 = 2\pi \cdot 17{,}3\,1/\text{s}$	$\omega_2 = 2\pi \cdot 30{,}6\,1/\text{s}$	$h_0 = 20\,\mu\text{m}$
$k_{1x} = k_{1y} = m_1\omega_1^2$	$k_{2x} = k_{2y} = m_2\omega_2^2$	$v = 800\,\text{m/min}$
$d_{1x} = d_{1y} = 400\,\text{Ns/m}$	$d_{2x} = d_{2y} = 400\,\text{Ns/m}$	$\mu = 0.5$
$r_1 = 0{,}345\,\text{m}$	$r_2 = 0{,}483\,\text{m}$	$k_{by} = 8.5 \cdot 10^{11}\,\text{N/m}$

Table 1: Parameters communicated by VAN HAAG (5)

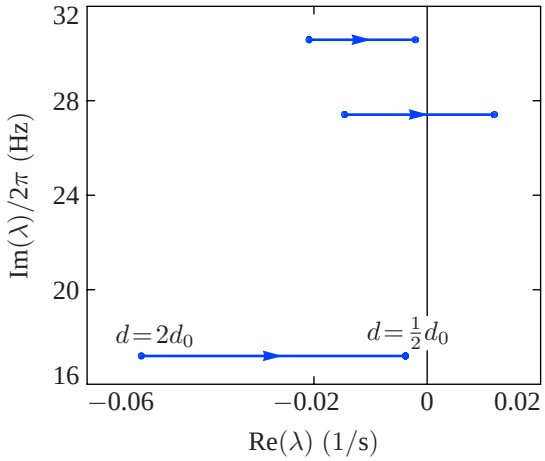

Figure 6: Eigenvalues of the system with two rigid rollers for varying damping in the bearings (d_0 refers to the nominal value given Table 1 and d is the actual value)

case that the upper roller is completely driven by the paper, whereas the lower roller drives the paper and therefore acts as a drive train for the calendering process. It is tacitly assumed that the neighboring calender stacks are controlled such that a constant paper velocity is maintained. For a linear elastic material law of the paper, the stress in the paper is given by

$$F_{\text{b}n}(s) = -k_{\text{b}y}\big(h(s) - h_0\big).$$

The linearized model can now be employed to draw the root locus of the system for varying parameters. From a variation of the damping in the bearings around $d_{1x} = d_{1y} = d_{2x} = d_{2y} = d_0$ (cf. Figures 6 and 7, d_0 being the reference value from table 1) it can be seen that higher damping in the bearings has a stabilizing effect, whereas the eigenfrequencies of the system remain almost unchanged. A variation of the paper bedding stiffness k_{by} around k_{by0} shows that higher stiffness has a destabilizing effect (Figure 8). Note that the system has another pair of

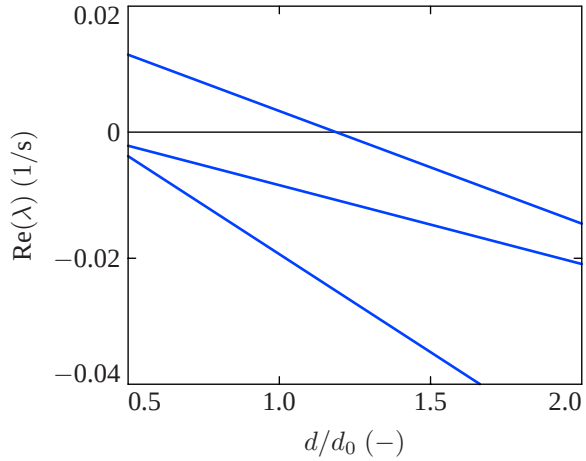

Figure 7: Real part of the eigenvalues of the system with two rigid rollers for varying damping in the bearings (d_0 refers to the nominal value given Table 1 and d is the actual value)

complex conjugate eigenvalues in the range of 200 Hz which has a negative real part and is omitted in the Figures

for presentation purposes.

Summarizing this section, the extension of the model including two rollers yields a self-excitation mechanism which is based on the frictional contact between the paper and the rollers and the plastic deformation of the paper. Due to the inextensibility assumption of the paper, there are no shear deformations in the paper, so that there is always slip (except at most at two single points) between the rollers and the paper. Similar friction-induced instability mechanisms are known from many other applications, as for example the squealing of brakes.

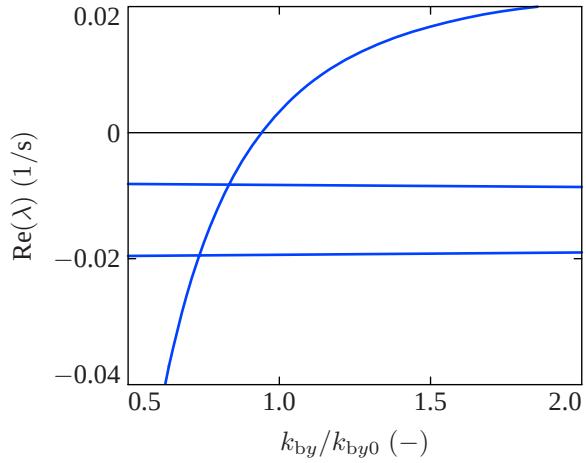

Figure 8: Real part of the eigenvalues of the system with two rigid rollers for varying paper stiffness (k_{by0} refers to the nominal value given Table 1 and k_{by} is the actual value)

4 Single roller with sticking condition

The assumption of inextensibility of the paper used in the last section is somewhat questionable, since the material properties of the paper are not known in much detail. The purpose of this section is to demonstrate that the excitation mechanism does not rely on the occurrence of slip between the rollers and the paper, but also occurs under the sticking condition. The analysis is based on the system shown in Figure 1. The paper model depicted in Figure 9 now includes extensibility in the horizontal direction, i.e. each material point characterized by the coordinate ξ in the undeformed configuration on the surface of the paper can undergo a displacement $u_1(\xi,t)$ parallel and a displacement $u_2(\xi,t)$ perpendicular to the mid surface of the paper, which as before is assumed to be inextensible and moves with constant velocity v. It is assumed that the paper and the roller stick together once contact is established. As in the previous sections, the paper is truncated at the narrowest point of the nip ($s=0$) and the deformation process is considered as quasi-stationary, since the transition through the nip happens on a much faster time scale than the vibration of the roller.

The forces acting in a paper element are proportional to its deformation. A paper element in contact with the roller at angle α has an upper point with position vector

$$\boldsymbol{p}_{\mathrm{u}} = (x - r\sin\alpha)\boldsymbol{e}_x + (y - r\cos\alpha)\boldsymbol{e}_y \tag{24}$$

and a lower base point at the mid surface of the paper given by

$$\boldsymbol{p}_{\mathrm{l}} = \left(x - r\sin\hat{\alpha} + v\,\frac{\hat{\alpha}-\alpha}{\Omega}\right)\boldsymbol{e}_x - (r+h_0)\boldsymbol{e}_y, \tag{25}$$

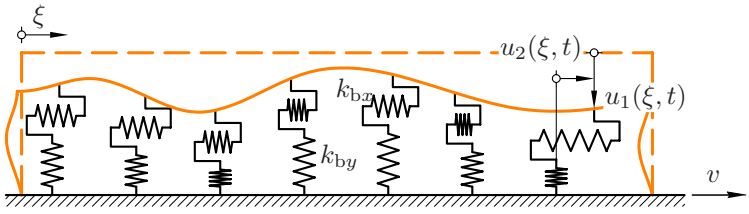

Figure 9: Paper model (extensible)

where the term $v(\hat{\alpha}-\alpha)/\Omega$ represents the distance the base point has traveled in $\boldsymbol{e}_x$-direction, while its counterpart on the roller traveled from $\hat{\alpha}$ to the position α. In correspondence with (3), the deformation in $\boldsymbol{e}_y$-direction is

$$\begin{aligned} h_1 - (\boldsymbol{p}_\mathrm{l} - \boldsymbol{p}_\mathrm{u}) \cdot \boldsymbol{e}_y &= h_1 - h_0 - r(1-\cos\alpha) + y \\ &= h_1 - h, \end{aligned} \tag{26}$$

whereas the deformation in $\boldsymbol{e}_x$-direction is

$$(\boldsymbol{p}_\mathrm{l} - \boldsymbol{p}_\mathrm{u}) \cdot \boldsymbol{e}_x = r(\sin\alpha - \sin\hat{\alpha}) + v\,\frac{\hat{\alpha}-\alpha}{\Omega} \tag{27}$$

due to the sticking condition between the paper and the roller. Referring to (4), $\hat{\alpha}$ is a function of y only, so that also the deformation of the paper is a function of y only. This is a consequence of the assumption of the quasi-stationary deformation process of the paper.

The equations of motion finally follow from NEWTON's law by summing up all forces acting on the roller

$$m\ddot{x} + k_x x = F_{x0} + \int_0^{\hat{\alpha}} k_{\mathrm{b}x} \left(r(\sin\alpha - \sin\hat{\alpha}) + v\,\frac{\hat{\alpha}-\alpha}{\Omega} \right) r\cos\alpha\,\mathrm{d}\alpha\,, \tag{28a}$$

$$m\ddot{y} + k_y y = F_{y0} + \int_0^{\hat{\alpha}} k_{\mathrm{b}y}\big(h_1 - h\big) r\cos\alpha\,\mathrm{d}\alpha\,. \tag{28b}$$

It should be noted that (28b) is identical to (7b). As for (7), the linearization of the equations of motion requires the application of LEIBNIZ's rule, because $\hat{\alpha}=\hat{\alpha}(y)$, and yields

$$\begin{bmatrix} m & 0 \\ 0 & m \end{bmatrix} \begin{bmatrix} \ddot{x} \\ \ddot{y} \end{bmatrix} + \begin{bmatrix} k_x & k_{\mathrm{b}x} r\, f_{k3} \\ 0 & k_y + k_{\mathrm{b}y} r \sin\hat{\alpha}_0 \end{bmatrix} \begin{bmatrix} x \\ y \end{bmatrix} = \begin{bmatrix} 0 \\ 0 \end{bmatrix} \tag{29}$$

with

$$\begin{aligned} f_{k3} &= -\frac{\mathrm{d}}{\mathrm{d}y} \int_0^{\hat{\alpha}(y)} \left(r(\sin\alpha - \sin\hat{\alpha}(y)) + v\,\frac{\hat{\alpha}(y)-\alpha}{\Omega} \right) \cos\alpha\,\mathrm{d}\alpha \Bigg|_{y=0} \\ &= 1 - \frac{h_1 - h_0}{r} - \frac{v}{\Omega r}\,. \end{aligned} \tag{30}$$

The present equations of motion for extensible paper with sticking condition are of the same mathematical form as for the inextensible paper with friction between the paper and the roller (10). Therefore, both systems show a similar stability behavior. In particular, instabilities arise for close eigenfrequencies of the system and small additional coupling of the equations. In both (10) and (29) the couplings f_{k2} and f_{k3} arise from the truncation at the end of the nip which can be seen as an effect of the plastic deformation of the paper. The term f_{k2} in (10) only contains an additional part originating from friction. The model with sticking condition can be easily extended to a two roller model similarly as done in the case of sliding friction. Due to the similarity of the equations in both cases, a qualitative change of the results is not to be expected. Therefore this step is not performed here.

5 Outlook and Conclusions

This paper deals with simple models for the explanation of self-excited vibrations of paper calenders. In contrast to most of the literature, the excitation mechanism studied in this paper does not rely on heuristic wear models leading to time delays in the equations of motion. Inspired by the papers of BROMMUNDT (3; 4) the excitation mechanism is explained by a refined modeling of the contact forces occurring in the nip which allow for a systematic stability analysis of the linearized equations of motion. Two sources of instability are identified, which are dry friction occurring in the slip regions, and plastic deformation of the paper as a second source. It is shown using rigid body models, that also in the case of pure sticking between the paper and the roller, self-excited vibrations can arise.

In future work the models presented will be extended allowing for elasticity of the rollers. A first step in this direction is to model the rollers as elastic rings and to assume point contact between the paper and the rollers. If slip between paper and rollers is assumed, the structure of the equations of motion is the same as for continuous models on brake squeal (6; 7). In order to model the excitation mechanism for self-excited vibrations also for sticking between rollers and paper a refined modeling with an extended nip similar to the analysis performed in section 4 will be required. The models presented in this paper may clear the way to a better understanding of self-excited vibrations in calenders and to an identification of critical design parameters using refined calender models. Such refined models should include coexisting sticking and slipping regions between the paper and the roller, and a physically justified model of the paper's plastic deformation.

References

[1] van Haag, R.: *Über die Druckverteilung und die Papierkompression im Walzenspalt eines Kalanders*, Ph.D. thesis, TU Darmstadt, 1993.

[2] Hader, P.: *Selbsterregte Schwingungen von Papierkalandern*, Ph.D. thesis, Universität Duisburg-Essen, 2005.

[3] Brommundt, E.: A simple model for friction induced high-frequency self-excitation of paper calenders, *Machine Dynamics Problems*, 31(2):25–45, 2007.

[4] Brommundt, E.: High-Frequency Self-Excitation in Paper Calenders, *Technische Mechanik*, 29(1):60–85, 2009.

[5] van Haag, R.: *Personal communication*, Krefeld, 2008.

[6] Hochlenert, D.; Spelsberg-Korspeter, G.; Hagedorn, P.: Friction Induced Vibrations in Moving Continua and Their Application to Brake Squeal, *Transactions of the ASME, Journal of Applied Mechanics*, 74:542–549, 2007.

[7] Spelsberg-Korspeter, G.; Kirillov, O.; Hagedorn, P.: Modeling and Stability Analysis of an Axially Moving Beam With Frictional Contact, *Journal of Applied Mechanics*, 75(3):031001/1–10, 2008.

Addresses: Dr.-Ing. Gottfried Spelsberg-Korspeter and Prof. Dr. Peter Hagedorn, System Reliability and Machine Acoustics, LOEWE-Zentrum AdRIA, Dynamics and Vibrations Group, Technische Universität Darmstadt.
email: speko@dyn.tu-darmstadt.de; hagedorn@dyn.tu-darmstadt.de
Dr.-Ing. Daniel Hochlenert, Institute of Mechanics, Chair of Mechatronics and Machine Dynamics, Technische Universität Berlin.
email: daniel.hochlenert@tu-berlin.de